



Catheter confocal fluorescence imaging and functional magnetic resonance imaging of local and systems level recovery in the regenerating rodent sciatic nerve

Galit Pelled, Stephen J. Dodd, and Alan P. Koretsky*

Laboratory of Functional and Molecular Imaging, National Institute of Neurological Disorders and Stroke, National Institute of Health, Bethesda, BID 728 10 Center Drive, MD 20892, USA

Received 13 July 2005; revised 14 October 2005; accepted 20 October 2005

The goal of the present work was to develop minimally invasive imaging techniques to monitor local regeneration of peripheral nerves and to determine the extent of return to function of brain cortical regions associated with that nerve. The sciatic nerve crush model was applied to Sprague–Dawley rats and conventional histological staining for myelin, axons and cell architecture was carried out, as well as traditional behavioral testing, to verify that nerve regeneration was occurring. The rate of sciatic nerve regeneration was measured by determining the distance a lipophilic, fluorescence probe (DiO) would move along the nerve's membrane following a direct injection into the sciatic nerve. This movement was monitored using a catheter based, confocal fluorescence microscope. Two to five days after the crush, the dye moved 1.4 ± 0.6 mm/day, as compared to a distance of 5.3 ± 0.5 mm/day in the normal nerve. Between 9 and 13 days following the crush, the distance the dye moved increases to 5.5 ± 0.5 mm/day, similar to the control, and by 15 days following the crush, the distance increased to 6.5 ± 0.9 mm/day. Functional Magnetic Resonance Imaging (fMRI) measurements were performed on α -chloralose anesthetized rats to monitor the return of somatosensory cortical functions, which were activated by the stimulation of the lesioned peripheral nerve. fMRI results showed the return of cortical activation around 15 days following the crush procedure. However, the somatosensory cortical region activated by stimulating the crushed hindpaw was significantly smaller in extent than the intact hindpaw stimulation. These findings demonstrate that fluorescence imaging and fMRI can integrate local and system level correlates of nerve regeneration in a non-destructive manner, thus enabling serial imaging of individual animals.

Published by Elsevier Inc.

Introduction

There is great interest in understanding and controlling the process of nerve regeneration. Peripheral nerves have the ability to regenerate following peripheral nerve trauma as long as the cell

bodies remain intact and the microenvironment at the site of the peripheral nerve permits delivery of essential growth factors to support the regrowing axons (Donnerer, 2003; Fu and Gordon, 1997; Ide, 1996; Terenghi, 1999; Zochodne, 2000). Much effort has been devoted to understand and facilitate the rate of nerve restoration and much has been learned about the cellular and molecular cascade of events that occur after peripheral nerve regeneration (Fu and Gordon, 1997; Ide, 1996; Terenghi, 1999). To integrate this information and to assess interventions, there is increasing need for techniques that can assess and monitor nerve regeneration in vivo. Invasive techniques, such as histology (Mackinnon et al., 1985), and retrograde labeling (Fink et al., 1987; Wikholm et al., 1988; Lozeron et al., 2004) have been the key techniques in order to assess nerve regeneration. Non-destructive techniques, such as behavioral methods (Ijkema-Paassen et al., 2004; Varejao et al., 2004), electrophysiology (Devor et al., 1979), microscopy (Shenag et al., 1989; Pan et al., 2003; Myckatyn et al., 2004) and magnetic resonance imaging (MRI) (Stanisz et al., 2001; Cudlip et al., 2002; Bendszus et al., 2004), provide essential information concerning peripheral nerve regeneration in experimental models. However, these measurements do not fully correlate with the return of motor and sensory functions (Munro et al., 1998; Dellon and Mackinnon, 1989) and do not allow both a high resolution view of local regeneration of damaged peripheral nerve as well as a systems level view of return of function.

At the level of the damaged nerve, peripheral nerves undergo a variety of structural and functional changes such as reduction in the number of cutaneous cell fibers (Wall and Devor, 1978), changes in axonal conduction velocity (Horch and Lisney, 1981; Mert et al., 2004), alternations in the topographical organization of nerves due to the growth of the regenerated nerves to abnormal skin locations and the extension of adjacent nerves into denervated areas (Devor et al., 1979; Horch, 1979; Streppel et al., 1998) and elevated tactile threshold (Terzis and Dykes, 1980). These changes served as the basis for developing methods to monitor regeneration. For example, electrophysiological methods can detect changes in nerve conduction and various MRI parameters have been shown to be

* Corresponding author. Fax: +1 301 480 2558.

E-mail address: KoretskyA@ninds.nih.gov (A.P. Koretsky).

Available online on ScienceDirect (www.sciencedirect.com).

effective in evaluating tissue damage and nerve regeneration processes in a non-invasive manner (Stanisz et al., 2001; Cudlip et al., 2002; Bendszus et al., 2004). While these methods provide localized information from the peripheral nerve, they do not predict the extent and the rate of the recovery of the entire neural system, including the return of cortical activity. Electrophysiological recordings from the brains of experimental animal models have demonstrated that peripheral regeneration results in reactivation of central circuits which enables cortical neurons to return to processing input from previously denervated regions (Wall et al., 1983, 1986; Murray et al., 1997). Although electrophysiological recordings are obtained with extraordinary spatial and temporal resolution, the limited number of cells which are examined and the invasive manner of the technique prevent it from becoming a routine method for evaluating cortical (or sub-cortical) recovery following peripheral nerve trauma.

The goal of the present work was to develop minimally invasive imaging techniques that monitor local regeneration of peripheral nerves at high resolution, as well as return to function of cortical regions that are activated by the stimulation of that peripheral nerve. The strategy was to apply functional MRI (fMRI), to monitor the return of cortical function, and catheter based confocal fluorescence microscopy to monitor local regeneration after a crush of the sciatic nerve. There is increasing interest in catheter based fluorescence microscopy to extend the type of imaging that can be done in conventional microscopes to tissue that cannot be easily placed in a microscope (Mehta et al., 2004). Recently, images with resolution down to a couple of microns were obtained both from the surface, as well as deep within a variety of tissues (Davenne et al., 2005; D'Hallewin et al., 2005; Laemmel et al., 2004; Rouse et al., 2004). The combination of these catheter based microscopy techniques and a wide range of fluorescent probes that are available to assess tissue anatomy and function make this an attractive choice for detecting local regeneration of peripheral nerves. Indeed, there has been work using more conventional microscopy studying mouse models expressing genetic encoded fluorescence protein to follow regeneration of a peripheral nerve (Pan et al., 2003; Myckatyn et al., 2004). To get a systems level view of regeneration, fMRI should be very useful. The fMRI signal is sensitive to changes in hemodynamics due to alterations in neuronal activity, through a complex cascade of events including changes in blood flow, blood volume and rate of oxygen utilization (Mandeville et al., 1998; Ogawa et al., 1992; Williams et al., 1992; Kim and Ugurbil, 1997) that occur due to neural stimulation. Currently, the most useful fMRI technique is based on the blood oxygenation level dependent (BOLD) contrast (Ogawa et al., 1992), where increase in the blood flow to an activated brain area results in an increase of the oxy/deoxyhemoglobin ratio in this area which leads to longer T2* or T2 and an increase in signal when the proper MRI sequence is used. Although BOLD fMRI provides an indirect measurement of neuronal activity, it has become a prominent tool for studying cortical activity in normal and pathological animal models (Dijkhuizen and Nicolay, 2003; Lythgoe et al., 2003; van der Weerd et al., 2004). New developments in fMRI of rodents permit spatial resolution of approximately 100 μm and temporal resolution for functional changes on the order of 100 ms (Silva and Koretsky, 2002; Keilholz et al., 2004), making MRI an emerging tool for studying brain reorganization processes in rodents. While fMRI has been applied to a very wide range of problems in the neurosciences, there have been no reports using fMRI to assess peripheral nerve regeneration.

In this work, we have applied the sciatic nerve crush model in rats, and implemented a multi-modal imaging approach to assess nerve regeneration and cortical recovery. To verify the model, traditional histological and behavioral methods were used. To assess the local regeneration of the sciatic nerve in vivo, catheter confocal microscopy was used with a fluorescent retrograde tracer to evaluate the rate of nerve regeneration. Finally, fMRI was used to non-invasively monitor the rate and the extent of cortical recovery and reorganization after regeneration of the sciatic nerve. The results indicate that the combination of fluorescence confocal catheter based microscopy and fMRI should lead to efficient and minimally invasive techniques to rapidly assess peripheral nerve regeneration.

Materials and methods

Overview of experiments

Overall, four types of methods were applied in order to evaluate the peripheral nerve regeneration process: histology, behavioral testing, optical imaging and fMRI. All of these experiments were carried out at three time periods for assessing structural and functional recovery during the initial, intermediate and final stages of nerve regeneration. The specific methods and the number of animals were as followed:

Initial stages following sciatic nerve crush (2–5 days post-crush): Behavioral testing ($n = 10$), catheter based confocal imaging with dye injected immediately following the crush ($n = 5$), fMRI measurements ($n = 6$), histology ($n = 6$).

Intermediate stages following sciatic nerve crush (9–13 days post-crush): Behavioral testing ($n = 6$), catheter based confocal imaging with dye injected at day 7, 9 and 11 following the crush ($n = 4$), fMRI measurements ($n = 4$).

Final stages following sciatic nerve crush (15–20 days post-crush): Behavioral testing ($n = 4$), catheter based confocal imaging with dye injected 15 days following the crush ($n = 6$), fMRI measurements ($n = 6$), histology ($n = 6$).

Animal model

All experiments were performed in compliance with guidelines set by the National Institutes of Neurological Disorders and Stroke ACUC. Male Sprague–Dawley rats were fed with RMH 1000 soy enriched protein diet a week prior to the surgeries and throughout the whole study. This diet has been previously shown to reduce post-operative pain (Shir et al., 2001). Rats (70–90 g, 4 weeks old (Harlen, IN)) were anesthetized with 2% isoflurane using a nose cone, and received a single dose of buprenorphine (0.02 mg/kg) prior and at the end of all surgical procedures.

The sciatic nerve was crushed with a 0.8 mm tip forceps for 20 s and a fine 5/0 silk suture (Stoelting, IL) was used to mark the crush site. These procedures were performed under microscopy guidance.

After surgery, the surgical site was closed using 9 mm EZ clips (Stoelting, IL) which were removed 7 days later. Rats were treated twice a day with Tramadol (1.5 ml/100 g) pain analgesia, and their weight, food consumption, posture, behavior and overall appearance were monitored daily. In addition, all rats were placed in an enriched environment (Playground kit (PetSmart, AZ)) for 3 h, four times a week.

Immediately after completing the MRI and optical imaging procedures and euthanizing the animals, a 1 mm section of the sciatic nerve 1 mm under the crush location was removed and placed in paraformaldehyde (Sigma, MO) for histology. Staining for myelin (Luxol fast blue), axons (Silver stain) and cell morphology (hematoxylin and eosin) were performed on 10 μm paraffin embedded coronal sections (Histoserve, MD).

Behavioral testing

A traditional hindpaw pinch test using fine forceps was applied in order to assess the behavioral outcome of the regenerating sciatic nerve. Rats were placed in a box with a gridded bottom which allowed access to the rostral part of the rats' hindpaw from below. The intact/crushed hindpaw was lightly pinch using 0.5 mm tip forceps for 5 s and the time it took the rats to retract its hindpaw was recorded.

Catheter confocal fluorescence microscopy

Detection of the membrane dye diffusion within the regenerated nerve was performed using a confocal, fiber optic based fluorescence microscope (Cell-Vizio, Mauna Kea Technologies, France). This system is composed of a laser scanning unit, with an excitation wavelength of 488 nm and a collection wavelength of 500–650 nm, 1.8 or 1.5 mm diameter flexible optical mini-probes, made from several 10 of thousands of single optical fibers as well as custom micro-optics, and an image analysis software. The 1.8 and 1.5 mm probes allowed an 80 μm working distance with a field of view of 240×170 and 425×323 μm , respectively. An image of a 15 μm thick slice within the sciatic nerve with a spatial resolution of 2.5×2.5 μm could be obtained. Images were sampled every 88 ms.

Two microliters of the lipophilic membrane tracer 5% DiO (Molecular probes, OR) in DMF was injected into the nerve bundle right above the crush site using a 33 gauge needle fitted in a 2.5 μl syringe (Hamilton, NV). The dye injection was performed either at the day of the crush and then imaged 2–5 days later, or 7, 9 and 11 days following the crush and imaged at days 9, 11 and 13, respectively. In addition, DiO was injected 15 days following the crush, and imaged 2 days later, in order to evaluate the dye movement during the final stages of nerve regeneration.

Rats were anesthetized with 2% Isoflurane using a nose cone, and 2.5 mm of the wound was reopened to allow insertion of the fiber optic probe. The probe was placed on the exposed sciatic nerve *in vivo*. The distance that the applied DiO moved within the regenerated nerve was evaluated with respect to the initial crush site. Since the DiO initial injection site was marked with the silk suture, the exact distance the dye had moved could be evaluated. After assessing the distance the dye had moved, the wound was closed using EZ clips and the animals were allowed to recover. Two-tailed Student's *t* test was performed between groups.

Functional MRI

Rats were initially anesthetized and maintained at 2% isoflurane during the following surgical procedures for MRI. Each rat was orally intubated and placed on a mechanical ventilator throughout the surgery and the experiment. Plastic catheters were inserted into the right femoral artery and vein to allow monitoring of arterial blood gases and administration of drugs. Two needle electrodes

were inserted just under the skin of each hindpaw, one between digits 1 and 2, and the other between digits 3 and 4. After surgery, the rat was given an i.v. bolus of α -chloralose (80 mg/kg (Sigma, MO)) and isoflurane was discontinued. Anesthesia was maintained with a constant α -chloralose infusion (27 mg/kg/h) and an i.v. injection of pancuronium bromide (4 mg/kg) was given once per hour to prevent motion (Silva and Koretsky, 2002; Keilholz et al., 2004).

The rat was placed on a heated water pad to maintain rectal temperature at 37°C while in the MRI. Each animal was secured in a head holder with ear bars and a bite bar to prevent head motion and was strapped to a plastic cradle. End-tidal CO₂, rectal temperature, tidal pressure of ventilation, heart rate and arterial blood pressure were continuously monitored during the experiment. Arterial blood gas levels were checked periodically and corrections were made by adjusting respiratory volume or administering sodium bicarbonate to maintain normal levels when required.

All images were acquired on an 11.7 T/31 cm horizontal bore magnet (Magnex, Abingdon, UK), interfaced to an AVANCE console (Bruker, Billerica, MA) and equipped with a 9-cm gradient set, capable of providing 64 G/cm with a rise time of 100 μs (Resonance Research, Billerica, MA). A 2 cm diameter surface coil that was attached to a head holder was used to transmit and receive the MR signal. Scout images were acquired in three planes with a fast spin echo sequence to determine appropriate positioning for the functional study. A single-shot, spin-echo echo-planar imaging (EPI) sequence with a 64×64 matrix was run with the following parameters: effective echo time (TE), 30 ms; repetition time (TR), 1.5 s; bandwidth, 200 kHz; and a field of view, 2.64×2.64 cm. Brain coverage was obtained with 5, 2-mm thick slices, spaced 0.2 mm apart.

A stimulator (World Precision Instruments, FL) supplied 2.5 mA, 300 μs pulses repeated at 3 Hz to either the right or the left hindpaws upon demand. The paradigm consisted of 10 dummy scans to reach steady state, followed by 40 scans during rest and 10 scans during hindpaw stimulation and was repeated at least 2 times. The animal was allowed to rest for few minutes between sets, and 3 to 5 sets of data were recorded from each animal for each of the hindpaws. Analysis of the fMRI time series was performed using STIMULATE (University of Minnesota, MN). A correlation coefficient was calculated from cross-correlation of the unfiltered time series with a boxcar waveform representing the stimulation period. The activation threshold was typically set at 0.22, and only groups that include at least four activated pixels were considered significant. The activation threshold was determined by the overall noise level in the EPI image. While 0.22 was the typical threshold that was used, in a few cases, activation outside the brain was still present and in these cases the threshold was increased up to 0.4 until the activation outside the brain was eliminated. The number of pixels above this threshold and their averaged amplitude was calculated for each data set. Two-tailed paired Student's *t* test was performed between groups.

Results

Gross behavior after the crush

The weight, posture, behavior and overall appearance of all the rats were monitored daily by the investigators and by blinded

observers. The rats were caged together (≥ 2 rats/cage) and were placed in an enriched environment in order to provide a variety of sensory and motor stimulators that would eventually encourage the regeneration rate (van Meeteren et al., 1997). In the days immediately following the surgery, the rats were dragging the hindpaw that had the sciatic nerve crushed. However, all rats remained active without experiencing any weight loss or self-mutilation (autotomy). Two weeks following the crush, the rats had improved their posture enormously, and flexion and extension of the hindpaw associated with the crush nerve were observed in all rats. This was an indication that at least partial regeneration of the sciatic nerve had occurred at this time point.

Histology

Following nerve trauma, peripheral nerves undergo Wallerian Degeneration processes, which involve a wide range of changes, from the cellular level to the level of gene expression (Stoll and Muller, 1999). This process has stereotypical morphological changes. Fig. 1 shows representative histological staining for cell morphology, myelin and axons of control, crushed and regenerated nerves. Indications of Wallerian Degeneration such as invasion of phagocytes, myelin swelling and axonal fragmentation can be clearly identified in the nerves that had been crushed as compared to control nerves. Two weeks after the crush, there were clear signs of regeneration of the sciatic nerve. The myelin appears to return to more normal architecture. However, there are still signs of swollen and fragmented cells as well as the presence of phagocytes in the regenerated nerve suggesting that the regeneration process was not complete at this time.

Behavior

Lightly pinching the rat's hindpaw caused immediate retraction of the intact hindpaw (<1 s, $n = 10$). At the days following the crush procedure, no retraction of the crushed hindpaw was observed

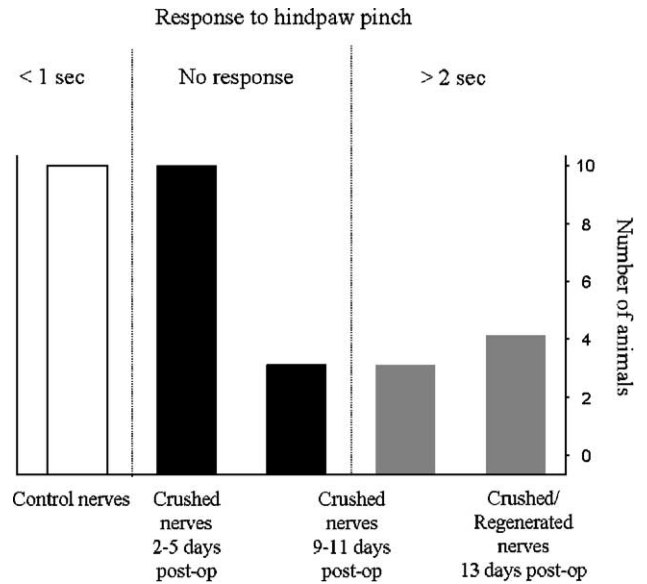


Fig. 2. The response of the crushed hindpaw (HP) to the pinch test which was performed at different time points following the crush procedure. Where the rats retract their intact HP immediately following a light pinch in the rostral part of the HP, retraction of the crushed HP was not observed within 5 days following the crush procedure. In the intermediate stages of nerve regeneration (9–11 days post-op), half of the rats showed no response to the pinch test, while the other half retract their HP slowly. In later stages of nerve regeneration (13 days post-op), all rats retracted their HP following the pinch, although continues pinching for few seconds was needed.

following 5 s of pinching (Fig. 2). In the period from 9 to 11 days following the crush procedure, half of the rats ($n = 3$) responded to hindpaw pinching by retracting their hindpaw, whereas the other half of the rats ($n = 3$) did not respond to the pinch at all. At this time point, rats who responded to the pinch retract their hindpaw with a

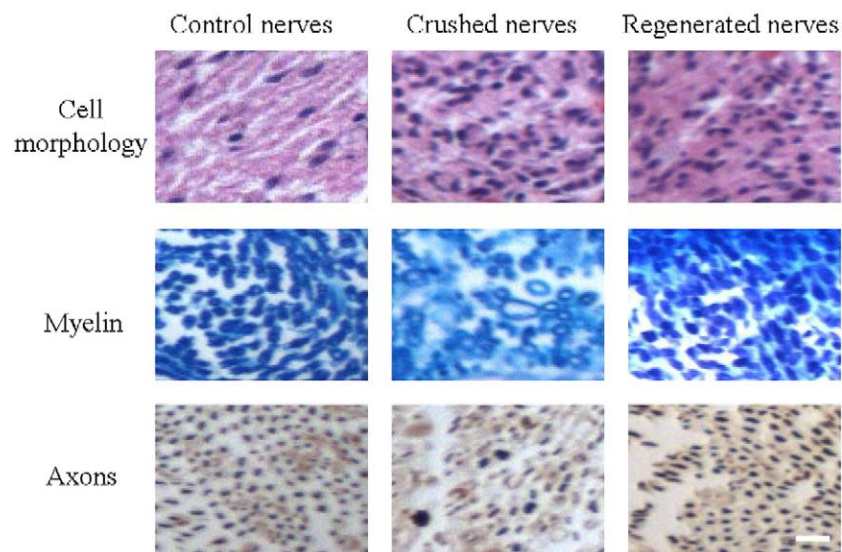


Fig. 1. Representative histological staining of control, crushed (2–5 days after crush) and regenerated (15–25 days after crush) coronal sciatic nerve sections. Staining for cell morphology (Hematoxylin and eosin), myelin (Luxol fast blue) and axons (Silver stain) were performed on 10 μ m coronal sections. As compared to the cell morphology, myelin and axons architecture of the intact nerves, Wallerian Degeneration markers as phagocytes, myelin and axonal fragmentation are clearly apparent at the first days following the nerve crush and 15–25 days following the nerve crush procedure. Scale bar corresponds to 10 μ m.

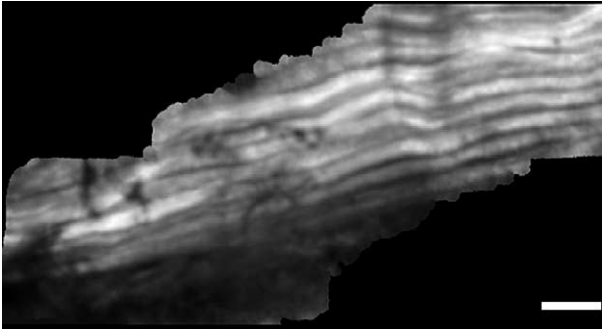


Fig. 3. Fluorescent DiO labeled nerves in the sciatic bundle of a control nerve using the catheter based, confocal microscope. The optic fiber probe was placed over the sciatic nerve and was slowly moved distally (about 10 mm) and the image was reconstructed from a series of single image, showing the length of the nerves. The field of view of the mosaic picture is 448×239 , and the scale bar corresponds to 1 mm.

greater delay compared to controls (>2 s). By 13 days following the crush, all rats responded to the pinch test and retracted their crushed (regenerated) hindpaw ($n = 4$). Delay in the hindpaw retraction was still present 13 days following the crush.

Catheter based confocal fluorescence imaging

The procedure of injecting the lipophilic neural track tracer DiO into the nerve and using a 1.8 or a 1.5 mm diameter optical fiber for imaging enabled a clear view of nerve bundles and quantification of the distance that the dye moved within the nerve. Ninety minutes after the dye application into control nerves, the dye was located within a radius of 0.5 mm around the injection site. Therefore, the injection pressure did not cause by itself any diffusion of the dye within the nerves' membrane.

Fig. 3 shows an image of approximately 1.5 cm of a labeled nerve. This image was made by tiling individual frames of a nerve by moving the probe down the length of the nerve. Two days after

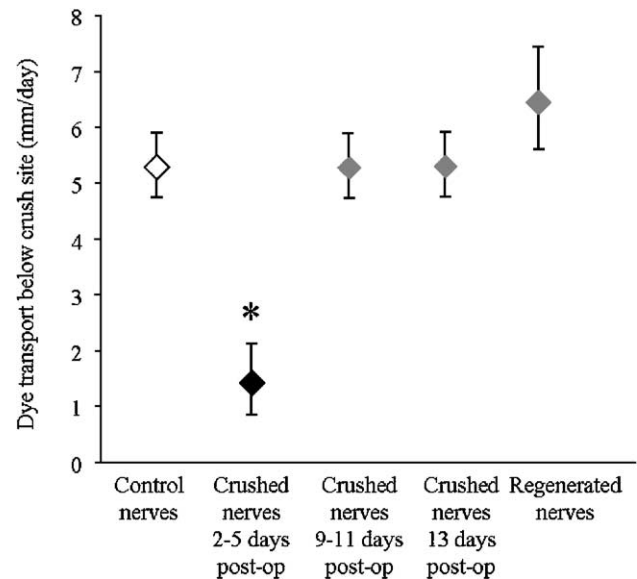


Fig. 5. The average diffusion distance of the lipophilic retrograde tracer DiO in control, crushed and regenerated nerves. Data were derived from images as shown in Fig. 2. Crushed nerves were imaged within 5, 9–11 and 13 days after the crush and regenerated nerves were imaged 15–20 days after the crush.

injection of DiO, fluorescence could be detected along the length of this nerve.

Fig. 4 shows representative fluorescence images of the control, crushed and regenerated sciatic nerve recorded from different locations beneath the crush site, 2 days after retrograde tracer injection. The control shows well ordered architecture of the neuronal bundles within the peripheral nerve. The farthest point fluorescence that could be detected was about 12 mm distal to the injection site 2 days after injection of DiO. Thus, the retrograde tracer moved 5.3 ± 0.5 mm/day in the control nerve (Fig. 5).

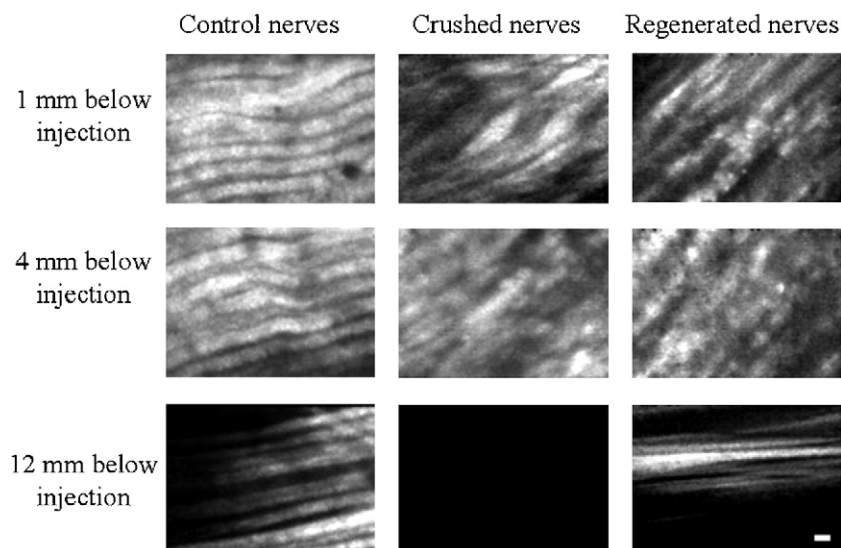


Fig. 4. Representative sagittal images taken with the catheter based, confocal microscope 2 days following injection of the lipophilic retrograde tracer DiO into control, crushed and regenerated nerves in vivo. The control nerve shows the normal architecture of several nerve bundles beneath the injection. Twelve millimeter below the injection was the furthest location that the fluorescent dye was detected. Uneven architecture and of the crushed and the regenerated nerves suggest pathological nerve conditions. Due to the short diffusion distance of the retrograde tracer, no fluorescent was detected at 12 mm below the injection site in the crushed nerve and only a few fibers could be detected this far in the regenerated nerve. Scale bar corresponds to 12 μ m.

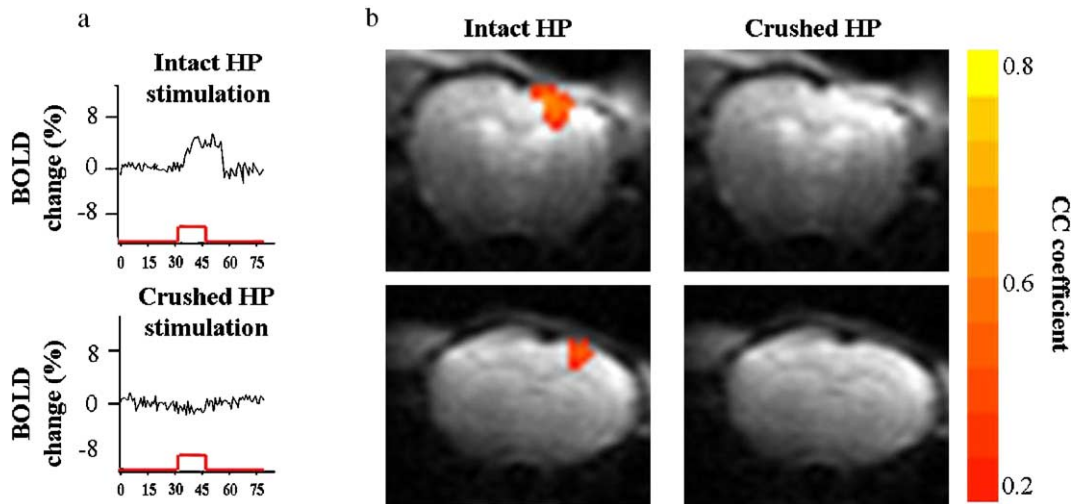


Fig. 6. Representative BOLD fMRI time courses and activation maps of control (intact HP) and crushed hindpaws (Crushed HP) 5 days following nerve crush procedure. (a) The averaged BOLD time course of the activated region when the sensory stimulation was applied to the intact or the crushed HP. The average time course for the somatosensory response following intact HP stimulation is plotted for all the activated pixels in the image. For the crushed HP, since no activating pixels were found, the time course of the BOLD signal within the somatosensory hindpaw representation, as was determined by a brain atlas, is plotted. The sensory stimulation paradigm is illustrated in the graph. (b) Two representative cross correlation (>0.22) activation maps from two different rats overlaid on an echo-planner spin echo image are shown. The somatosensory response of the intact hindpaw stimulation is demonstrated in the left column and lack of somatosensory response to the crushed hindpaw stimulation is demonstrated in the right column. Due to the complete loss of afferent input from the sciatic nerve, somatosensory cortical activation is not detected at this initial stage of regeneration.

Fig. 4 shows that the appearance of the nerve bundles in the crushed nerve was much less uniform than in control nerves indicating that that myelin swelling and fragmentation influenced the image of DiO (Stoll and Muller, 1999; Koeppen, 2004). The neuronal tracer moved within the crushed nerve only 1.4 ± 0.6 mm/day with similar values measured during the first 5 days following the crush. Due to the short distance the tracer tracked in the crushed nerve, no fluorescence signal was detected 10 mm beneath the injection site during the first 5 days (Fig. 4).

In order to image more advanced regenerating neurons, the retrograde tracer was injected above the crushed site on days 7, 9 and 11 following the crush. Starting at the ninth day following the crush, the retrograde tracer was found to move a distance of 5.5 ± 0.5 mm/day, similar to control nerves. Later stages of regeneration were studied after applying the retrograde tracer at day 15 and imaging the nerve 17 days following crush. Fig. 4 shows that fragmented and patchy neuronal architecture was still present, consistent with the histological findings. Even though the appearance of the tissue at 17

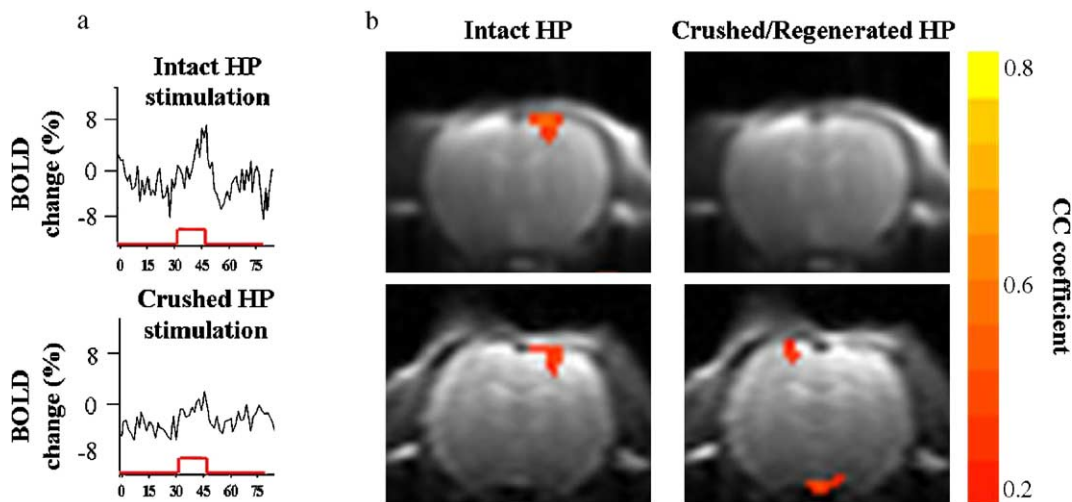


Fig. 7. Representative BOLD time course and activation maps of intact and crushed/regenerated hindpaws (HP) 9 and 11 days following nerve crush procedure. (a) The averaged BOLD time course of the activated region when the sensory stimulation was applied to the intact or the regenerated HP 11 days after the sciatic nerve crush. The average time course is plotted for all the activated pixels in the image. The sensory stimulation paradigm is illustrated in the graph. (b) Two representative cross correlation (>0.22) activation maps from two different rats overlaid on an echo-planner spin echo image are shown. The somatosensory response of the intact hindpaw stimulation is demonstrated in the left column and somatosensory response to the crushed hindpaw stimulation is demonstrated in the right column. On the top, fMRI activation maps were acquired 9 days following the crush, and on the bottom, 11 days later. Whereas no activation was found in the somatosensory cortex 9 days following crush following crushed HP stimulation, the activation is back after 11 days.

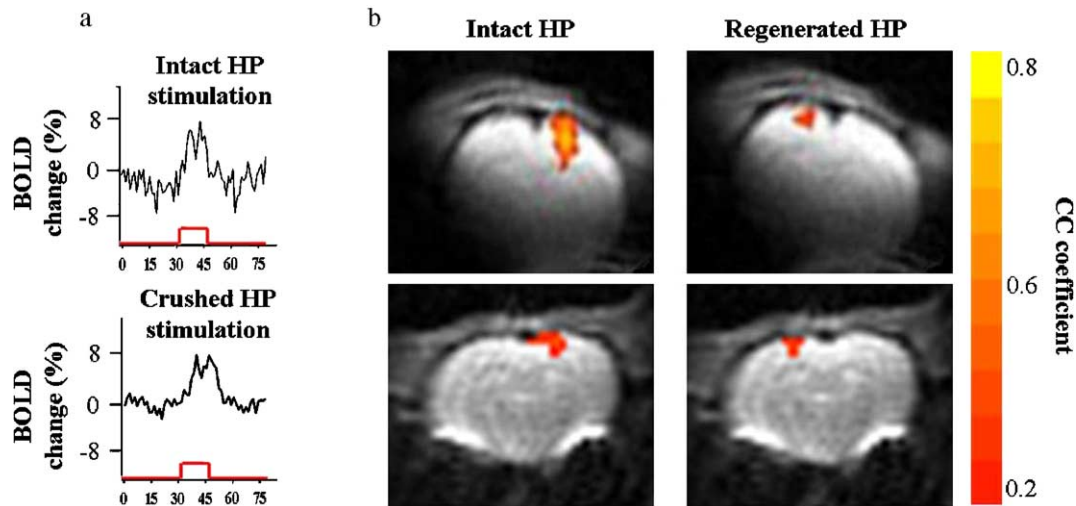


Fig. 8. Representative BOLD time course and activation maps of intact and regenerated hindpaws (HP) 20 days following nerve crush procedure. (a) The averaged BOLD time course of the activated region when the sensory stimulation was applied to the intact or the regenerated HP. The average time course is plotted for all the activated pixels in the image. The sensory stimulation paradigm is illustrated in the graph. (b) Two representative cross correlation (>0.22) activation maps from two different rats overlaid on an echo-planner spin echo image are shown. The somatosensory response of the intact hindpaw stimulation is demonstrated in the left column and somatosensory response to the crushed hindpaw stimulation is demonstrated in the right column. These activation maps represent the second stage of cortical recovery, whereas there is restoration of the somatosensory cortical representation. The example in the top panel demonstrates the reduced number of activated pixels corresponding to the sensory stimulation of the regenerated HP compared to the intact HP.

days was more similar to the crushed than the control nerve, the distance that the retrograde tracer moved within the regenerated nerve was similar to that of the control nerve (6.5 ± 0.9 mm/day). Thus, both the structural features of the fluorescence images as well as the distance traveled by the DiO gave indications of damage and recovery from the crush.

Functional MRI

In order to evaluate whether response of somatosensory cortex recovered during regeneration of sciatic nerve, fMRI experiments were carried out. Figs. 6–8 demonstrate representative BOLD activation maps overlaid on the EPI images used to generate the activation maps from 2 different rats. Also shown are representative time courses showing the fMRI response to the stimulation. As expected, sensory stimulation that was applied to the intact (left)

hindpaw at any time point after the crush procedure led to activation in the contralateral somatosensory cortex. No cortical activation was observed when stimulating the crushed hindpaw 3–7 days following the crush procedure (Fig. 6). Fig. 7 shows activation maps which correspond to intermediate stages of nerve regeneration. Whereas 3 rats did not show any cortical activation in response to stimulation of the crushed hindpaw, one rat showed partial recovery of the sciatic nerve, as could be derived by the activation observed contralateral to the crushed hindpaw. Fig. 8 shows that 15 to 20 days following the crush procedure, there was a return of somatosensory cortical activation when the contralateral, crushed nerve was stimulated. This indicates that by this time regeneration had occurred to restore system level function of the sciatic nerve.

Although sensory stimulation of the regenerated hindpaw resulted in detectable cortical fMRI activation after 15–20 days, the cortical area activated was significantly smaller compared to

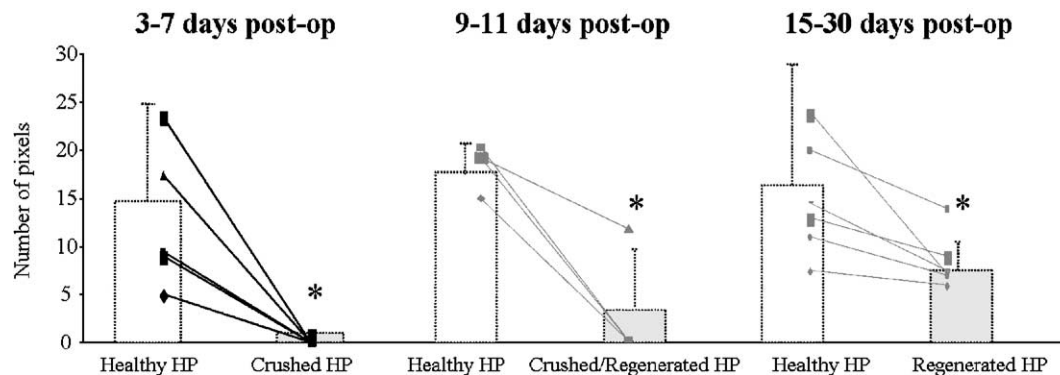


Fig. 9. The group averaged and single rat comparison of the number of activated pixels in the somatosensory cortex resulting with sensory stimulation of the intact and the crushed/regenerated hindpaws (HP). Functional MRI performed on rats 3–7 days following the nerve crush procedure (3–7 post-op) shows no significant number of activated pixels corresponding to stimulation of the crushed HP in all the rats tested (left). During the regeneration process (9–11 days post-op), most of the rats did not show any activation resulting from crushed HP stimulation, except from one rat. During recovery (15–30 days post-op), there was restoration of the somatosensory representation in all animals (right). In 5 out of the 6 rats tested at this time point, there was a reduction in the somatosensory representation in the regenerated nerve cortex with respect to the control side ($*P < 0.05$).

stimulation of the intact hindpaw within the same rats. Fig. 9 shows the individual rats and group average comparison of the number of activated pixels above the cross-correlation threshold used when stimulating the intact and the crushed/regenerated hindpaws. The size of the somatosensory cortical area that activated when the intact hindpaw was stimulated was on average 50% larger than the size of the cortical representation detected from the hindpaw 15 days after nerve crush (Fig. 9). For the pixels that activated, there was no significant difference in the BOLD amplitude between groups and within an animal ($P > 0.5$).

Discussion

The goal of this work was to determine if minimally invasive imaging could be used to assess regeneration of sciatic nerve both at a local level and at the level of system function. Catheter based, confocal fluorescence microscopy of nerve stained with the lipophilic nerve tracer DiO enabled visualization of nerve bundles and measurement of regeneration, while fMRI enabled assessment of information flow to the cortex during regeneration.

Histological staining carried out at different time points after the sciatic nerve crush procedure confirmed that Wallerian Degeneration followed by nerve regeneration was taking place in the model used in a manner consistent with previous studies (Stoll and Muller, 1999; Koeppen, 2004). In addition, conventional behavioral testing paradigm was applied in order to correlate imaging results with the behavioral outcome. In order to visualize in vivo the rate of nerve regeneration, we applied a catheter confocal fluorescence microscopy of DiO injected nerves, which allowed longitudinal investigation of the regeneration process with minimal physiological discomfort. DiO is widely used as anterograde and retrograde neuronal tracers in living (Honig and Hume, 1989) and fixed (Godement et al., 1987) tissues and cells. The dye labels uniformly neurons via lateral diffusion in the plasma membrane at a rate of about 6 mm per day due to active dye transport processes (Honig and Hume, 1989). The rate of nerve regeneration during the first few days after the nerve crush procedure was assessed by the distance DiO traveled. This distance was approximately 1.5 mm/day, in agreement with previous studies that relied on excised tissue (Sjoberg and Kanje, 1990). The distance the tracer moved was found to increase to approximately 5 mm/day about 1 week after the nerve crush. This is also consistent with previous studies (Sjoberg and Kanje, 1990; IJkema-Paassen et al., 2004; Lozeron et al., 2004). Therefore, catheter based confocal fluorescence microscopy of DiO injected fibers led to a minimally invasive assessment of peripheral nerve regeneration.

Recently, nerve regeneration following crush was studied using fluorescence microscopy in transgenic mice expressing fluorescent proteins whose expression was controlled using a neuron specific promoter. In these mice models, all the peripheral neurons expressed the fluorescent protein, therefore, quantification of the number of regenerated axons and their rate of regeneration could be specifically addressed (Pan et al., 2003; Myckatyn et al., 2004). A drawback of this approach is that it requires an animal model that expresses fluorescent proteins. Here, we used direct injection of the fluorescent dye, DiO, into the peripheral nerve to overcome the need to express fluorescent proteins. This enabled the assessment of the anatomy of the nerve bundles as well as the rate of transport of the indicator in a rat model and should be applicable to a wide range of animal models. While the distance

that the DiO moved was quantified, no attempt was made to quantify the number of fiber bundles that had regenerated. One problem with making such quantification is that the injection procedure did not always uniformly label the nerve most likely due to limitations of the injection technique and washout of the DiO. Furthermore, with the catheter probe used, it was difficult to acquire data through the full thickness of the nerve. It should be possible to solve these problems to enable quantitative counting of intact nerve bundles. Imaging through the entire peripheral nerve has been accomplished with confocal fluorescence microscopy (Myckatyn et al., 2004; Pan et al., 2003). Furthermore, there are a wide variety of fluorescent agents available that should enable monitoring many aspects of both Wallerian Degeneration and return to function, such as selectively labeling immune cells to assess inflammation and monitoring calcium transients in the nerve with fluorescent calcium dyes.

While histological and optical imaging techniques offer the ability to examine the series of cellular processes taking place during nerve regeneration, neither methods supply information about restoration of nerve function. Indeed, one of the goals of the peripheral nerve research field is to develop anatomical and functional measures to evaluate restoration of nervous system function. fMRI is an excellent method that enables detection of aspects of neural activation throughout the brain with good temporal resolution and excellent spatial resolution in a non-invasive manner. There have been a large number of fMRI studies to localize functions in the brain and to study plasticity and recovery from central nervous system injury. To the best of our knowledge, the present work is the first that uses fMRI to assess the return of cortical activity during regeneration after injury of a peripheral nerve.

Both optical imaging and fMRI identified two stages of recovery. Initially, the nerve crush procedure caused large disruption in the anatomy of the sciatic nerve, very short distances DiO moved and a complete lack of sciatic nerve afferent information to the brain as indicated by lack of the somatosensory cortical fMRI activation when the hindpaw was stimulated. Sometime after the first week following the nerve crush, the distance DiO moved returned close to control levels as the nerve regenerates during the second phase of recovery. It is interesting to note that, during the intermediate stages of nerve regeneration (9–11 days following sciatic nerve crush) whereas the distance of DiO movement was close to control values, the behavioral assessment as well as cortical fMRI activation still showed lack of functional recovery of the injured hindpaw. Therefore, these results suggest that the anatomical recovery which seems to be rapid at this time point is followed by much slower functional restoration of the hindpaw.

The first time point where the second stage of nerve regeneration leads to recovery of cortical activity was about 2 weeks following the nerve crush procedure. This corresponded to the time when rats exhibit an improvement in posture, behavior and partial return of hindpaw functionality, as could be derived by the behavioral tests. However, the extent of cortical activation remained smaller than control for up to 3 weeks, the longest time studied. It will be interesting to see if there is a gradual return of activation of the entire cortical representation over a long time interval. Furthermore, it will be interesting to correlate the number of regenerated fibers with the extent of cortical activation. The ability to measure these parameters in the same animal, serially over time will make these quantitative studies possible.

The reason that activation of the entire hindpaw representation did not return is not clear. The most likely explanation is that not all nerve fibers have fully regenerated consistent with the optical imaging data showing a smaller number of fibers containing DiO far from the crush site as compared to controls. It may also be that there are other factors. During nerve regeneration, several processes have been shown to take place that could interfere with restoring normal somatosensory activation. The saphenous nerve, which is the adjacent nerve to the sciatic nerve, could innervate areas that have been previously innervated by the sciatic nerve (Devor et al., 1979), the regenerated nerves could fail to reinnervate the correct area (Horch, 1979; Streppel et al., 1998) and the receptive field of the neurons in the spinal cord and the cortex could expand (Devor and Wall, 1981; Devor et al., 1979; Wall et al., 1986). These alternations in peripheral and central neurons could directly affect return of normal cortical organization.

In conclusion, it has been demonstrated that both local correlates of peripheral nerve regeneration and system level correlates of peripheral nerve regeneration could be obtained either non-invasively or in a minimally invasive manner with a combination of optical microscopy and fMRI. The use of a newly available catheter based confocal fluorescence microscope enabled rapid monitoring of the regeneration of the peripheral nerve and fMRI enabled monitoring of the return of cortical activity. In agreement with previous studies, 2 weeks after traumatizing the sciatic nerve, the rats exhibited regeneration processes that were detected by the optical imaging. In addition, the fMRI results suggest that the rate and the extent of cortical recovery follow a similar time course. These findings demonstrate that fluorescence imaging and fMRI can integrate local and system level correlates of nerve regeneration in a non-destructive manner enabling serial imaging of individual animals. This should enable more efficient assessment of regeneration for studying the basic biology of regeneration as well as studying the efficacy of therapeutic interventions.

Acknowledgments

The authors would like to thank Torri Wilson and Kathryn Sharer for animal preparation and physiology. This work was supported by the NINDS intramural research program, Henry McFarland, Acting Scientific Director.

References

- Bendszus, M., Wessig, C., Solymosi, L., Reiners, K., Koltzenburg, M., 2004. MRI of peripheral nerve degeneration and regeneration: correlation with electrophysiology and histology. *Exp. Neurol.* 188, 171–177.
- Cudlip, S.A., Howe, F.A., Griffiths, J.R., Bell, B.A., 2002. Magnetic resonance neurography of peripheral nerve following experimental crush injury, and correlation with functional deficit. *J. Neurosurg.* 96, 755–759.
- Davenne, M., Custody, C., Charneau, P., Lledo, P.M., 2005. In vivo imaging of migrating neurons in the mammalian forebrain. *Chem. Senses* 30 (Suppl. 1), i115–i116.
- Dellon, A.L., Mackinnon, S.E., 1989. Selection of the appropriate parameter to measure neural regeneration. *Ann. Plast. Surg.* 23, 197–202.
- Devor, M., Wall, P.D., 1981. Plasticity in the spinal cord sensory map following peripheral nerve injury in rats. *J. Neurosci.* 1, 679–684.
- Devor, M., Schonfeld, D., Seltzer, Z., Wall, P.D., 1979. Two modes of cutaneous reinnervation following peripheral nerve injury. *J. Comp. Neurol.* 185, 211–220.
- D'Hallewin, M.A., El Khatib, S., Leroux, A., Bezdetnaya, L., Guillemin, F., 2005. Endoscopic confocal fluorescence microscopy of normal and tumor bearing rat bladder. *J. Urol.* 174, 736–740.
- Dijkhuizen, R.M., Nicolay, K., 2003. Magnetic resonance imaging in experimental models of brain disorders. *J. Cereb. Blood Flow Metab.* 23, 1383–1402.
- Donnerer, J., 2003. Regeneration of primary sensory neurons. *Pharmacology* 67, 169–181.
- Fink, D.J., Purkiss, D., Mata, M., 1987. Retrograde axonal transport in rat sciatic nerve after nerve crush injury. *Brain Res. Bull.* 19, 29–33.
- Fu, S.Y., Gordon, T., 1997. The cellular and molecular basis of peripheral nerve regeneration. *Mol. Neurobiol.* 14, 67–116.
- Godement, P., Vanselow, J., Thanos, S., Bonhoeffer, F., 1987. A study in developing visual systems with a new method of staining neurones and their processes in fixed tissue. *Development* 101, 697–713.
- Honig, M.G., Hume, R.I. 1989. Dil and diO: versatile fluorescent dyes for neuronal labelling and pathway tracing. *Trends Neurosci.* 12, 333–335, 340–341.
- Horch, K., 1979. Guidance of regrowing sensory axons after cutaneous nerve lesions in the cat. *J. Neurophysiol.* 42, 1437–1449.
- Horch, K.W., Lisney, S.J., 1981. On the number and nature of regenerating myelinated axons after lesions of cutaneous nerves in the cat. *J. Physiol.* 313, 275–286.
- Ide, C., 1996. Peripheral nerve regeneration. *Neurosci. Res.* 25, 101–121.
- Ijkema-Paassen, J., Jansen, K., Gramsbergen, A., Meek, M.F., 2004. Transection of peripheral nerves, bridging strategies and effect evaluation. *Biomaterials* 25, 1583–1592.
- Keilholz, S.D., Silva, A.C., Raman, M., Merkle, H., Koretsky, A.P., 2004. Functional MRI of the rodent somatosensory pathway using multislice echo planar imaging. *Magn. Reson. Med.* 52, 89–99.
- Kim, S.G., Ugurbil, K., 1997. Comparison of blood oxygenation and cerebral blood flow effects in fMRI: estimation of relative oxygen consumption change. *Magn. Reson. Med.* 38, 59–65.
- Koeppen, A.H., 2004. Wallerian degeneration: history and clinical significance. *J. Neurol. Sci.* 220, 115–117.
- Laemmel, E., Genet, M., Le Goualher, G., Perchant, A., Le Gargasson, J.F., Vicaut, E., 2004. Fibered confocal fluorescence microscopy (Cell-viZio) facilitates extended imaging in the field of microcirculation. A comparison with intravital microscopy. *J. Vasc. Res.* 41, 400–411.
- Lozeron, P., Krarup, C., Schmalbruch, H., 2004. Regeneration of unmyelinated and myelinated sensory nerve fibres studied by a retrograde tracer method. *J. Neurosci. Methods* 138, 225–232.
- Lythgoe, M.F., Sibson, N.R., Harris, N.G., 2003. Neuroimaging of animal models of brain disease. *Br. Med. Bull.* 65, 235–257.
- Mackinnon, S.E., Hudson, A.R., Hunter, D.A., 1985. Histologic assessment of nerve regeneration in the rat. *Plast. Reconstr. Surg.* 75, 384–388.
- Mandeville, J.B., Marota, J.J., Kosofsky, B.E., Keltner, J.R., Weissleder, R., Rosen, B.R., Weisskoff, R.M., 1998. Dynamic functional imaging of relative cerebral blood volume during rat forepaw stimulation. *Magn. Reson. Med.* 39, 615–624.
- Mehta, A.D., Jung, J.C., Flusberg, B.A., Schnitzer, M.J., 2004. Fiber optic in vivo imaging in the mammalian nervous system. *Curr. Opin. Neurobiol.* 14, 617–628.
- Mert, T., Daglioglu, Y.K., Gunay, I., Gocmen, C., 2004. Changes in electrophysiological properties of regenerating rat peripheral nerves after crush injury. *Neurosci. Lett.* 363, 212–217.
- Munro, C.A., Szalai, J.P., Mackinnon, S.E., Midha, R., 1998. Lack of association between outcome measures of nerve regeneration. *Muscle Nerve* 21, 1095–1097.
- Murray, G.M., Taub, D.R., Mackie, P.D., Zhang, H.Q., Ghosh, S., Rowe, M.J., 1997. The effects of neonatal median nerve injury on the responsiveness of tactile neurones within the cuneate nucleus of the cat. *J. Physiol.* 505 (Pt. 3), 759–768.
- Myckatyn, T.M., Mackinnon, S.E., Hunter, D.A., Brakefield, D., Parsadanian, A., 2004. A novel model for the study of peripheral-nerve

- regeneration following common nerve injury paradigms. *J. Reconstr. Microsurg.* 20, 533–544.
- Ogawa, S., Tank, D.W., Menon, R., Ellermann, J.M., Kim, S.G., Merkle, H., Ugurbil, K., 1992. Intrinsic signal changes accompanying sensory stimulation: functional brain mapping with magnetic resonance imaging. *Proc. Natl. Acad. Sci. U. S. A.* 89, 5951.
- Pan, Y.A., Misgeld, T., Lichtman, J.W., Sanes, J.R., 2003. Effects of neurotoxic and neuroprotective agents on peripheral nerve regeneration assayed by time-lapse imaging in vivo. *J. Neurosci.* 23, 11479–11488.
- Rouse, A.R., Kano, A., Udovich, J.A., Kroto, S.M., Gmitro, A.F., 2004. Design and demonstration of a miniature catheter for a confocal microendoscope. *Appl. Opt.* 43, 5763–5771.
- Shenaq, S.M., Mendelow, M., Shenaq, J.M., Spira, M., 1989. Evaluation of axonal specificity of the regenerating rat sciatic nerve using a fluorescent labeling technique. *Microsurgery* 10, 210–213.
- Shir, Y., Raja, S.N., Weissman, C.S., Campbell, J.N., Seltzer, Z., 2001. Consumption of soy diet before nerve injury preempts the development of neuropathic pain in rats. *Anesthesiology* 95, 1238–1244.
- Silva, A.C., Koretsky, A.P., 2002. Laminar specificity of functional MRI onset times during somatosensory stimulation in rat. *Proc. Natl. Acad. Sci. U. S. A.* 99, 15182–15187.
- Sjoberg, J., Kanje, M., 1990. The initial period of peripheral nerve regeneration and the importance of the local environment for the conditioning lesion effect. *Brain Res.* 529, 79–84.
- Stanisz, G.J., Midha, R., Munro, C.A., Henkelman, R.M., 2001. MR properties of rat sciatic nerve following trauma. *Magn. Reson. Med.* 45, 415–420.
- Stoll, G., Muller, H.W., 1999. Nerve injury, axonal degeneration and neural regeneration: basic insights. *Brain Pathol.* 9, 313–325.
- Streppel, M., Angelov, D.N., Guntinas-Lichius, O., Hilgers, R.D., Rosenblatt, J.D., Stennert, E., Neiss, W.F., 1998. Slow axonal regrowth but extreme hyperinnervation of target muscle after suture of the facial nerve in aged rats. *Neurobiol. Aging* 19, 83–88.
- Terenghi, G., 1999. Peripheral nerve regeneration and neurotrophic factors. *J. Anat.* 194 (Pt. 1), 1–14.
- Terzis, J.K., Dykes, R.W., 1980. Reinnervation of glabrous skin in baboons: properties of cutaneous mechanoreceptors subsequent to nerve transection. *J. Neurophysiol.* 44, 1214–1225.
- van der Weerd, L., Thomas, D.L., Thornton, J.S., Lythgoe, M.F., 2004. MRI of animal models of brain disease. *Methods Enzymol.* 386, 149–177.
- van Meeteren, N.L., Brakkee, J.H., Hamers, F.P., Helders, P.J., Gispen, W.H., 1997. Exercise training improves functional recovery and motor nerve conduction velocity after sciatic nerve crush lesion in the rat. *Arch. Phys. Med. Rehabil.* 78, 70–77.
- Varejao, A.S., Melo-Pinto, P., Meek, M.F., Filipe, V.M., Bulas-Cruz, J., 2004. Methods for the experimental functional assessment of rat sciatic nerve regeneration. *Neurol. Res.* 26, 186–194.
- Wall, P.D., Devor, M., 1978. *Physiology of Sensation After Peripheral Nerve Injury, Regeneration, And Neuroma Formation*. Raven, New York.
- Wall, J.T., Felleman, D.J., Kaas, J.H., 1983. Recovery of normal topography in the somatosensory cortex of monkeys after nerve crush and regeneration. *Science* 221, 771–773.
- Wall, J.T., Kaas, J.H., Sur, M., Nelson, R.J., Felleman, D.J., Merzenich, M.M., 1986. Functional reorganization in somatosensory cortical areas 3b and 1 of adult monkeys after median nerve repair: possible relationships to sensory recovery in humans. *J. Neurosci.* 6, 218–233.
- Wikholm, R.P., Swett, J.E., Torigoe, Y., Blanks, R.H., 1988. Repair of severed peripheral nerve: a superior anatomic and functional recovery with a new “reconnection” technique. *Otolaryngol.-Head Neck Surg.* 99, 353–361.
- Williams, D.S., Detre, J.A., Leigh, J.S., Koretsky, A.P., 1992. Magnetic resonance imaging of perfusion using spin inversion of arterial water. *Proc. Natl. Acad. Sci. U. S. A.* 89, 212–216.
- Zochodne, D.W., 2000. The microenvironment of injured and regenerating peripheral nerves. *Muscle Nerve, Suppl.* 9, S33–S38.